Stiffness Characteristics Analysis of a Novel 3-DOF Parallel Kinematic Machine Tool

Haiqiang Zhang and Hairong Fang

***Abstract*—A novel 1T2R with three degrees of freedom redundantly actuated and overconstrained 2RPU-2SPR parallel manipulator is here presented as an alternative approach for high speed machining in aerospace field. Firstly, the actuation and constraints of the parallel manipulator imposed by passive joints are analyzed in terms of the screw theory, and the degree of freedom of the parallel manipulator is further derived. Secondly, the kinematic analysis is carried out, the inverse position and geometric constraint equations of the parallel manipulator are established, and the overall Jacobian matrix was explicitly derived. Subsequently, the stiffness matrix of the chain is deduced considering the elastic deformation of the link, and the stiffness matrix of the parallel manipulator is established by the differential mapping relationship between the actuated chains and the moving platform. The linear and angular stiffness, eigenscrew decomposition, and maximum and minimum stiffness eigenvalues are introduced to evaluate the stiffness characteristics of the manipulator. Finally, through some numerical examples, distributions law of the performance indices of redundantly actuated and overconstrained 2-RPU-2SPR parallel manipulator are illustrated in details. The results demonstrate that the three degree of freedom redundant actuation parallel manipulator proposed in this paper has much better stiffness performance than the 2-RPU-SPR parallel manipulator, and has much more extensive prospect in engineering applications.**

***Index Terms*—Redundantly actuated, overconstrained, parallel manipulator, eigenscrew, stiffness.**

I. Introduction

In recent years, lower degree of freedom (DOF) parallel manipulator especially 1T2R with three DOFs parallel manipulator as the main body of the high-end intelligent equipment is the focus of the current trend, which has been demonstrated by abundant engineering applications in the aerospace field for complex component machining, such as Sprint Z3 spindle [1], Tricept hybrid machine tool [2], Exechon hybrid machine tool [3], etc. In practical applications, to increase the workspace of 1T2R parallel manipulator, a hybrid structure is generally derived by integrating a serial model with a parallel manipulator. At the same time, to improve the orientation capability of the end effector, two or three degrees of freedom rotating head can be attached on the moving platform, so the multi-degree of freedom hybrid machine tool can be constructed. In view of structural component with large dimension and complex freedom surface in aerospace field, a novel 1T2R lower DOF parallel manipulator with higher stiffness and higher orientation capability is of great importance kernel issue by adding two tracks in *X-Y* axis to form five axis serial-parallel hybrid machine tool to complete machining milling with high efficiency and high accuracy. Therefore, overconstrained parallel manipulator as a special lower DOF parallel manipulator came into being in this mode, which can effectively avoid the singularity, increase the workspace, and improve kinematics and dynamic characteristics, enlarge stiffness and driving stability, and so on. What's more, it has been successfully received extensive attentions in different engineering and technological areas as a special lower DOF parallel manipulator [4]-[6].

Up to now, most of the investigations can be focus on stiffness characteristics issue of the parallel kinematic machine (PKM). Domestic and foreign scholars have done numerous efforts on the stiffness of the parallel manipulators, and the main methods include analytical method and finite element method (FEM). For example, Gosselin firstly put forward a stiffness model for full degree of freedom planner and spatial mechanism based on the principle of virtual work, but this method only considered the stiffness of actuation joint, not considered constraint force and moment imposed by passive joint [7]. Clinton employed sub-structural matrix method to establish the stiffness analytical model for Gough-Stewart parallel manipulator to evaluate its stiffness performance [8]. A comprehensive stiffness modeling method was first proposed by Robert in virtue of the screw theory, who established the stiffness model including tension/compression, torsion, and deflection as well coupling, and the whole stiffness model was obtained by equivalent stiffness for linear connected springs in series [9]. Zhao investigated the overall stiffness matrix based on the virtual work principle by considering the actuation force, constraint force and virtual joint [10]. Zhang adopted virtual joint method to formulate the stiffness matrix of constrained parallel manipulator in which a weighted function could be maximized in terms of the main diagonal elements of the stiffness matrix. However, the value of trace of the stiffness matrix does not definitely predict the stiffness performance of the manipulator [11]. The stiffness of the Stewart parallel machine has been intensively investigated by Khasawneh [12],

Manuscript received December 5, 2017; revised March 21, 2018. This work was supported by the Central Universities under Grant No.2017YJS158.

Haiqiang Zhang is with School of Mechanical, Electronic and Control Engineering, Beijing Jiaotong University, Beijing, P.R. China (e-mail: 16116358@bjtu.edu.cn).

Hairong Fang is with Beijing Jiaotong University and Robotics Research Center Leader, P.R. China (e-mail: hrfang@bjtu.edu.cn).

DOI: 10.7763/IJET.2018.V10.1082

among others, whose approach is based on the generalized Jacobian matrix in terms of the minimum and maximum singular value of the stiffness to reveal the distribution, and simultaneously the static stiffness model of the end effector at different positions was established by using the finite element software. Wang performed parameterization model in virtue of commercial finite element software ANSYS, researched finite element modeling method of various joints, and demonstrated the stiffness performance of the five degrees of freedom Trivariant hybrid robot [13]. The stiffness modeling of redundant actuated and overconstrained parallel manipulator is still rarely seen. Yan and Li only analyzed the structural characteristics and freedom, and inverse and forward kinematics of the two overconstrained 2RPU&SPR parallel manipulator [14]. Zhang utilized the virtual joint method (VJM) to establish the stiffness model of chains and joints, and then the sub-structure synthesis method was employed to synthesize the static stiffness analytic model of the overconstrained Exechon parallel module, and the stiffness distribution over the prescribed workspace was further studied [15]. Cui established the chain stiffness and mechanism stiffness of 3RPS-UPS parallel manipulator based on the screw theory and illustrated the stiffness improvement owing to the actuation redundancy [16].

In summary, the structure of the paper is as follows: The structure of a novel redundantly actuated and overconstrained 2RPU-2SPR parallel kinematic machine tool is described, and the degree of freedom is further obtained considering the actuation force and constraint force/moment in terms of the screw theory in Section II. The kinematic analysis of the parallel manipulator, as well as the inverse position solution and the constraint equations, are carried out in Section III. The overall stiffness of the parallel manipulator is straightforward obtained considering tension compression, bending and torsion deformation of the links without considering the joints deformation in Section IV. The stiffness performance indices including linear and angular stiffness, stiffness eigenscrew decomposition, and maximum and minimum stiffness eigenvalue are introduced, the theoretical model proposed in this paper is verified by means of the FEA model, and the stiffness characteristics of the parallel manipulator was evaluated in Section V. Finally the conclusions are drawn, and demonstrate the merits of the proposed manipulator.

II. Degree of Freedom Analysis of the 2RPU-2SPR Parallel Manipulator

A. Architecture Description of the Manipulator

The parallel kinematic machine tool for high speed machining milling considered in this paper is shown in Fig.1 and the topological structure of its core module a novel redundantly actuated and overconstrained 2-RPU-2SPR parallel manipulator, is shown in Fig.2. The parallel module is comprised of the fixed platform attached to the moving platform through two identical revolute- prismatic- universal (RPU) joints in series and two identical spherical- prismatic-revolute (SPR) joints in series respectively and the prismatic joint is active joint which is actuated by the linear servo motor. Two RPU chains distribute symmetrically, and are located in the plane Ω . Similarly, the two SPR chains are also symmetrical distribution and located in the plane Π .The spindle tool is attached on the end of moving platform for the high speed milling machining.

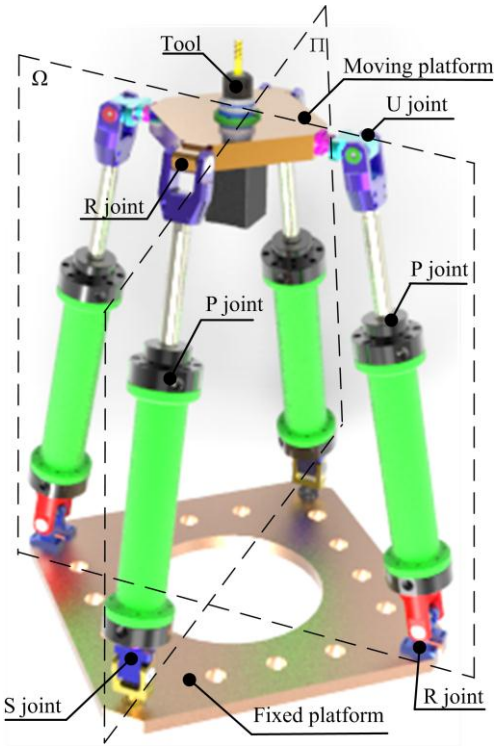

Fig. 1. The virtual prototype.

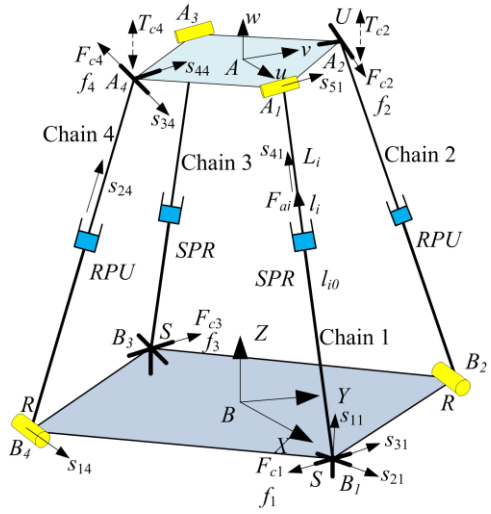

Fig. 2. The schematic diagram of the parallel manipulator

To facilitate analysis, the absolute coordinate system $B-xyz$ and the relative coordinate system $A-uvw$ are established as shown in Fig. 2. Wherein B is the midpoint of the fixed platform, the X axis is coincides with the vector BB_1, the Y axis is coincide with the vector BB_2, and the Z axis is perpendicular to the fixed platform upwards. Similarity, A is the midpoint of the moving platform, the u axis is coincides with the vector AA_1, the v axis is coincides with the vector AA_2, w axis is perpendicular to the moving platform upwards. In the SPR chains (taking the first chain as an example), the first rotation axis s_{11} of the spherical joint is

parallel to the *Z* axis, the second axis s_{21} is perpendicular to s_{11}, and the third rotation axis s_{31} is perpendicular to s_{41} and parallel to the rotation axis s_{51}. Similarity, in the RPU chains (taking the fourth chain as an example), the rotation joint axis s_{14} is parallel to the *X* axis, the universal joint consists of two vertical R joints, and the first rotation axis s_{34} is parallel to s_{14}, and the second rotation axis s_{44} is perpendicular to s_{34} and parallel to *v* axis.

B. Degree of Freedom Analysis of the Manipulator

According to the screw theory twist and wrench observation method, the 1, 2, 3, 4 chain provide actuation force F_{ai}, and its direction along the link l_{i0}. The 1 and 3 chain produce a constraint force F_{ci}, whose direction is parallel to *v* axis passing through the spherical joint (*i*=1, 3). The 2 and 4 chain produce a constraint force F_{ci} and a constraint moment T_{ci}, whose constraint force direction is parallel *X* axis passing through the universal joint and constraint moment direction is normal to the rotation axis of the universal joint (*i*=2, 4). The direction of constraint force imposed by passive joints denotes as f_i, and direction of constraint moment represents as τ_i [17]. It is known that the instantaneous constraint force and constraint moment don't work on the center of the moving platform in terms of screw theory, that is,

$$\begin{cases} F_{ci}\cdot f_i\cdot v+F_{ci}\cdot((a_i-l_i)\times f_i)\cdot w=0(i=1,3) \\ F_{ci}\cdot f_i\cdot v+F_{ci}\cdot(a_i\times f_i)\cdot w=0(i=2,4) \end{cases} \tag{1}$$

$$T_{ci}\cdot\tau_i\cdot w=0(i=2,4) \tag{2}$$

Rewriting Eqs.(1) and (2) in matrix form results in

$$\mathbf{J}_c\begin{bmatrix} v \\ \omega \end{bmatrix}=\begin{bmatrix} f_i^{\mathrm{T}} & ((a_i-l_i)\times f_i)^{\mathrm{T}} \\ f_i^{\mathrm{T}} & a_i\times f_i^{\mathrm{T}} \\ 0_{3\times1}^{\mathrm{T}} & \tau_i^{\mathrm{T}} \end{bmatrix}\begin{bmatrix} v \\ \omega \end{bmatrix}=0 \tag{3}$$

where $\mathbf{J}_c$ can be expanded as the follows

$$\mathbf{J}_c=\begin{bmatrix} f_1^{\mathrm{T}} & ((a_1-l_1)\times f_1)^{\mathrm{T}} \\ f_2^{\mathrm{T}} & a_2\times f_2^{\mathrm{T}} \\ f_3^{\mathrm{T}} & ((a_3-l_3)\times f_3)^{\mathrm{T}} \\ f_4^{\mathrm{T}} & a_4\times f_4^{\mathrm{T}} \\ 0_{3\times1}^{\mathrm{T}} & \tau_2^{\mathrm{T}} \\ 0_{3\times1}^{\mathrm{T}} & \tau_4^{\mathrm{T}} \end{bmatrix} \tag{4}$$

Due to the special configuration of the revolute joints, there are three linearly independent items in the constraint Jacobian matrix $\mathbf{J}_c$, so the mechanism has three redundant constraints, and the formula is based on the degree of freedom [18]

$$F=d(n-g-1)+\sum_{i=1}^{g}f_i+v-\varsigma \tag{5}$$

where *F* represents the degree of freedom of the mechanism, *n* represents the number of the components, *g* represents the number of the kinematic joints, $d=6-\lambda$ represents the order of the mechanism, fi represents the degree of freedom of the *i*-th kinematic joint, *v* represents the redundant constraints of the mechanism, and ς represents the local degree of freedom.

Neither constraint couple in the same direction, nor constraint force in collinear among the constraint screw in the parallel manipulator, therefore, there is no common constraint, that is, $\lambda=0$. Due to without local degree of freedom, so $\varsigma=0$. We can see from the schematic of the mechanism, the number of the component is 10, the number of the kinematic joint is 12, and the relative freedom of all the kinematic joints in the mechanism is 18, the degree of freedom of the 2-PRU-2SPR parallel manipulator can be mathematically calculated by applying the modified G-K equations, that is

$$F=6\times(10-12-1)+18+3-0=3 \tag{6}$$

According to the constraint force and moment, the independent degree of freedom is a translation that perpendicular to the constraint force F_{ci} and two rotations that perpendicular to the constraint moment T_{ci}. Because the mechanism has four active prismatic joint, so the mechanism belongs to redundantly actuated and overconstrained parallel manipulator.

III. Kinematic Analysis

A. Position Inverse Analysis

Z-Y-X Euler angles are adopted to describe orientation matrix of the moving coordinate system with respect to the absolute coordinate system, first rotating the moving platform about *z*-axis by angle γ , then about *y*-axis of the new coordinate system by angle β , and finally about *x*-axis of the new coordinate system by angle α. Thus, the orientation transformation matrix $\mathbf{R}$ can be written as follows

$$\begin{aligned}\mathbf{R}&=\mathbf{R}(\gamma,z)\mathbf{R}(\beta,y)\mathbf{R}(\alpha,x)\\&=\begin{bmatrix} c\beta c\gamma & s\alpha s\beta c\gamma-c\alpha s\gamma & c\alpha s\beta c\gamma+s\alpha s\gamma \\ c\beta s\gamma & s\alpha s\beta s\gamma+c\alpha c\gamma & c\alpha s\beta s\gamma-s\alpha c\gamma \\ -s\beta & s\alpha c\beta & c\alpha c\beta \end{bmatrix}\end{aligned} \tag{7}$$

where *s* and *c* are the abbreviation of *sine* and *cosine*, respectively.

$p=\begin{bmatrix} x & y & z \end{bmatrix}^T$ represents the position vector of the original point *A* in the absolute coordinate system . a_i and b_i represent the position vector in the absolute coordinate of joints A_i and B_i, $\square B_1B_2B_3B_4$ and $\square A_1A_2A_3A_4$ are both square whose circumradius are nominated as r_a , r_b , and the coordinate of each joint in the absolute coordinate system can be respectively expressed as

$$a_i=\mathbf{R}\begin{pmatrix} r_ac\theta_i & r_as\theta_i & 0 \end{pmatrix}^T,\quad b_i=\begin{pmatrix} r_bc\theta_i & r_bs\theta_i & 0 \end{pmatrix}^T \tag{8}$$

where $\theta_i=\dfrac{2(i-1)\pi}{4}, i=1,2,3,4$

In virtue of the arrangement of the revolute joints, the four constraint conditions can be structured as

$$\begin{cases} (p-b_i)^T\cdot\mathbf{R}\begin{pmatrix} 0 & 1 & 0 \end{pmatrix}^{\mathrm{T}}=0(i=1,3) \\ (p+a_i)^T\cdot\begin{pmatrix} 1 & 0 & 0 \end{pmatrix}^{\mathrm{T}}=0(i=2,4) \end{cases} \tag{9}$$

Selecting parameters α , β , z as three independent parameters, parasitic motion can be arranged as

$$x=0\,,\quad y=-\frac{zs\alpha c\beta}{s\alpha s\beta s\gamma+c\alpha c\gamma}\,,\quad \gamma=\arctan\left(\frac{s\alpha s\beta}{c\alpha}\right) \tag{10}$$

The close-loop vector method is used to establish the equation of vector A_iB_i in the absolute coordinate system $B-xyz$

$$\mathbf{L}_i=\mathbf{p}+\mathbf{a}_i-\mathbf{b}_i \tag{11}$$

Dot-multiplying Eq.(11) with itself, we yields by taking square root

$$l_i=\sqrt{(\mathbf{p}+\mathbf{a}_i-\mathbf{b}_i)(\mathbf{p}+\mathbf{a}_i-\mathbf{b}_i)} \tag{12}$$

B. The Jabobian Matrix of the Manipulator

If the velocity vector *v* and angular velocity vector *w* of the moving platform reference point *A* are known, the velocity vector v_{ai} of the joint point A_i that connected the actuated chain and moving platform can be expressed as

$$v_{ai}=v+\omega\times a_i\quad (i=1,2,3,4) \tag{13}$$

Then the velocity $\dot{l}_i$ of the *i*-th linear actuator can be expressed as

$$\dot{l}_i=v_{ai}\cdot l_{i0}=(v+\omega\times a_i)\cdot l_{i0} \tag{14}$$

The Eq.(14) can be written in the matrix form

$$\dot{l}_i=\mathbf{J}_a\begin{bmatrix}v\\ \omega\end{bmatrix},\quad \mathbf{J}_a=\begin{bmatrix}l_{i0}^T & (a_i\times l_{i0})^T\end{bmatrix} \tag{15}$$

Where $\mathbf{J}_a$ presents the actuation Jacobian matrix of the parallel manipulator.

Thus, combining Eq.(4) and Eq.(15)can be rewritten in the matrix form

$$\dot{l}_i=\mathbf{J}_0\begin{bmatrix}v\\ \omega\end{bmatrix},\quad \mathbf{J}_0=\begin{bmatrix}\mathbf{J}_a\\ \mathbf{J}_c\end{bmatrix} \tag{16}$$

where $\mathbf{J}_0$ is the generalized Jacobain matrix of the parallel manipulator that relates the velocity of joint to the velocity of the moving platform.

According to the dual relationship between the velocity mapping and the force mapping, the relation between the chains and the moving platform can be obtained by Eq.(17)

$$\tau=\mathbf{J}_0^{\,T}f\,,\quad \tau=\begin{bmatrix}F^T & M^T\end{bmatrix}^T,\ f=\begin{bmatrix}f_a^T & f_c^T\end{bmatrix}^T \tag{17}$$

Where τ presents the external force *F* and external moment *M* acting on the reference point at the moving platform, and *f* presents driving force f_a and constraint force f_c of the kinematic chains.

IV. Stiffness Modeling of the Manipulator

Without the loss of generality, when constructing the stiffness analytic model of redundantly actuated and overconstrained parallel manipulator, it was explicitly assumed that the moving and fixed platforms are perfectly rigid, ignoring the deformation of the rotational joint, spherical joint and universal joint, and only considering the elastic deformation of the links. The actuation force, constraint force and amplitude exerted to the moving platform can be denoted as $\$_{ai}$, f_{ai} and $\$_{ri}$, f_{ri} (i=1,2,3,4)respectively. The second and fourth chain can provide the moving platform with constraint moment and amplitude $\$_{\tau i}$, $f_{\tau i}$ (i=2, 4), it can be also decomposed into two constraint moments along the driving link and perpendicular to the driving link direction [19].

A. Stiffness Modeling of the Chain

The chain will produce tensile deformation under driving force screw $\$_{ai}$, f_{ai} , that is

$$f_{ai}=k_{ai}\delta_{ai}\,,\ k_{ai}=\frac{EA}{l_i} \tag{18}$$

where *E* is the elasticity modulus, *A* is the cross-section of the link, and k_{ai} is the tension/compression stiffness coefficient of the link.

The deflection δ_{ri} of the link along the constraint force axis under constraint force screw $\$_{ri}$, f_{ri} can be expressed as

$$f_{ri}=k_{ri}\delta_{ri}\,,\quad k_{ri}=\frac{3EI_z}{l_i^{\,3}} \tag{19}$$

where I_z is the section inertia moment, and k_{ri} is bending stiffness coefficient.

The deflection $\delta\theta_{i1}$ along the link axis under constraint moment screw $\$_{\tau j}$, $f_{\tau j}$ can be denoted as

$$f_{\tau i}\tau_i l_{i0}=k_{ni}\delta\theta_{i1}\,,\quad k_{ni}=\frac{GI_p}{l_i} \tag{20}$$

where *G* is shear modulus, I_p is polar inertia moment, $\tau_i=e_1\times e_2$, $e_1=\begin{pmatrix}1 & 0 & 0\end{pmatrix}^{\mathrm{T}}$,and $e_2=R\begin{pmatrix}1 & 0 & 0\end{pmatrix}^{\mathrm{T}}$.

Similarly, the deflection $\delta\theta_{i2}$ of perpendicular the link axis under constraint moment screw $\$_{\tau j}$, $f_{\tau j}$ can be indicated as

$$f_i\tau_i(e_1\times l_{i0})=k_{ti}\delta\theta_{i2}\,,\quad k_{ti}=\frac{EI_z}{l_i} \tag{21}$$

A matrix form can be written as

$$\begin{bmatrix}f_{ai} & f_{ri} & f_{\tau j}\end{bmatrix}^{\mathrm{T}}=\mathbf{K}_0\begin{bmatrix}\delta_{ai} & \delta_{ri} & \delta_{\theta j1} & \delta_{\theta j2}\end{bmatrix}^{\mathrm{T}}\ i=1,2,3,4,\ j=2,4) \tag{22}$$

where,

$$\mathbf{K}_0=\begin{bmatrix}\mathbf{K}_a & \mathbf{0}_{4\times4} & \mathbf{0}_{4\times4}\\ \mathbf{0}_{4\times4} & \mathbf{K}_c & \mathbf{0}_{4\times4}\\ \mathbf{0}_{2\times4} & \mathbf{0}_{2\times4} & \mathbf{K}_\tau\end{bmatrix},\ \mathbf{K}_a=\mathrm{diag}\begin{bmatrix}k_{a1} & k_{a2} & k_{a3} & k_{a4}\end{bmatrix},$$

$$\mathbf{K}_c=diag\begin{bmatrix}k_{r1} & k_{r2} & k_{r3} & k_{r4}\end{bmatrix},\mathbf{K}_\tau=\begin{bmatrix}\mathbf{K}_{\tau1} & \mathbf{0}_{1\times2}\\ \mathbf{0}_{1\times2} & \mathbf{K}_{\tau2}\end{bmatrix},$$

$$\mathbf{K}_{\tau 1}=\begin{bmatrix}\dfrac{k_{n2}}{\tau_2 l_{20}+\tau_2(e_1\times l_{20})} & \dfrac{k_{t2}}{\tau_2 l_{20}+\tau_2(e_1\times l_{20})}\end{bmatrix},$$

$$\mathbf{K}_{\tau 2}=\begin{bmatrix}\dfrac{k_{n4}}{\tau_4 l_{40}+\tau_4(e_1\times l_{40})} & \dfrac{k_4}{\tau_4 l_{40}+\tau_4(e_1\times l_{40})}\end{bmatrix}$$

B. Stiffness Model of the Parallel Manipulator

The mapping relationship between actuation chains deformation and moving platform displacement ΔX can be expressed as

$$\begin{bmatrix}\delta_{ai} & \delta_{ri} & \delta_{\theta j1} & \delta_{\theta j2}\end{bmatrix}^{\mathrm{T}}=\mathbf{J}_v\Delta X \tag{23}$$

Where $\mathbf{J}_v=\begin{bmatrix}\mathbf{J}_a\\ \mathbf{J}_{rc}\\ \mathbf{J}_{\tau c}\end{bmatrix}$, $\mathbf{J}_{rc}=\mathbf{J}_c(1:4,1:6)$,

$$\mathbf{J}_{\tau c}=\begin{bmatrix}\mathbf{0}_{3\times1}^{\ T} & l_{20}^{\ T}\\ \mathbf{0}_{3\times1}^{\ T} & (e_1\times l_{20})^T\\ \mathbf{0}_{3\times1}^{\ T} & l_{40}^{\ T}\\ \mathbf{0}_{3\times1}^{\ T} & (e_1\times l_{40})^T\end{bmatrix}$$

Substituting Eqs. (22) and (23)to Eq.(17), we can obtain the equation

$$\tau=\mathbf{J}_0^T\mathbf{K}_0\mathbf{J}_v\Delta X \tag{24}$$

The stiffness matrix of the parallel manipulator can be rewritten as

$$\mathbf{K}=\mathbf{J}_0^{\ T}\mathbf{K}_0\mathbf{J}_v \tag{25}$$

V. Stiffness Performance Indices

A. Linear Stiffness and Angular Stiffness

If the structural parameters and pose are given, the stiffness matrix of the parallel manipulator will be determined. Some stiffness performance indices can be defined to evaluate the stiffness characteristics. Here we treat the diagonal corresponding element of the stiffness matrix as the linear stiffness and angular stiffness, which can be defined in details as follows [20]-[21].

$$\begin{cases}k_x=\mathbf{K}(1,1)\\ k_y=\mathbf{K}(2,2)\\ k_z=\mathbf{K}(3,3)\\ k_w=\mathbf{K}(6,6)\end{cases} \tag{26}$$

where k_x, k_y and k_z are the linear stiffness along X-,Y-, and Z-axis, respectively; k_w is the torsional stiffness about *Z*-axis.

Once the parameters of geometry, configuration and physical are given in Table I, the stiffness matrix under the configuration can be derived as follows Eq.(25)

TABLE I: Related Parameters of Manipulator

Type	Parameter	Value
Structure	r_a(/*mm*)	278
	r_b(/*mm*)	565
	l_i(/*mm*)	(750,1250)
Pose	α (/*radian*)	0
	β (/*radian*)	0
	z(/*mm*)	853
Physical	E(/*Pa*)	2.06x10^{11}
	G(/*Pa*)	7.69x10^{10}
	A(/m^2)	7.06 x10^{-4}
	I_z(/m^4)	3.97 x10^{-8}

The stiffness matrix of the home position configuration can be obtained

$$\mathbf{K}=\begin{bmatrix}0.3297 & 0 & 0 & 0 & 0.2719 & 0\\ 0 & 0.3297 & 0 & -0.2713 & 0 & -0.0006\\ 0 & 0 & 5.8136 & 0 & 0 & 0\\ 0 & -0.2713 & 0 & 0.2252 & 0 & -0.0005\\ 0.2719 & 0 & 0 & 0 & 0.2248 & 0\\ 0 & -0.0006 & 0 & -0.0005 & 0 & 0.0008\end{bmatrix}\times10^8 \tag{27}$$

where the units of terms are N/m for $\mathbf{K}_{11}$, $\mathbf{K}_{22}$, and $\mathbf{K}_{33}$, and Nm/rad for $\mathbf{K}_{44}$, $\mathbf{K}_{55}$, and $\mathbf{K}_{66}$.

With the help of commercial finite element software AnsysWorkbench, the validity of the stiffness model is verified, finite element analysis of the PKM is conducted at the specified configuration [22]. For facilitate analysis, the finite element model of the virtual prototype is constructed for the home position in the workspace, the deformations of the parallel manipulator under force or moment are shown in Fig. 3. Fig. 3a-3c illustrated the deformation of the parallel manipulator under force along the direction of *X*-axis, *Y*-axis, and *Z*-axis, respectively. Fig.3d demonstrated the deformation of the parallel manipulator under the moment about the direction of *Z*-axis.

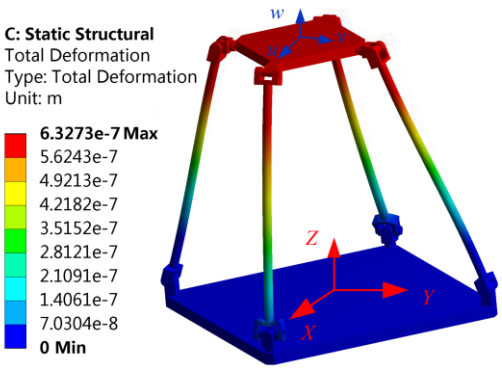

(a) Deformation along *X*-axis under F=[20N,0,0]$^{\mathrm{T}}$

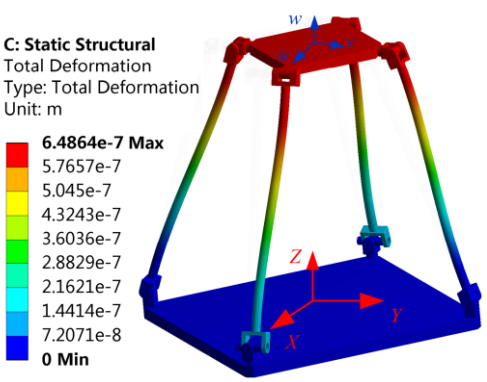

(b) Deformation along *Y*-axis under F=[0,20N,0]$^{\mathrm{T}}$

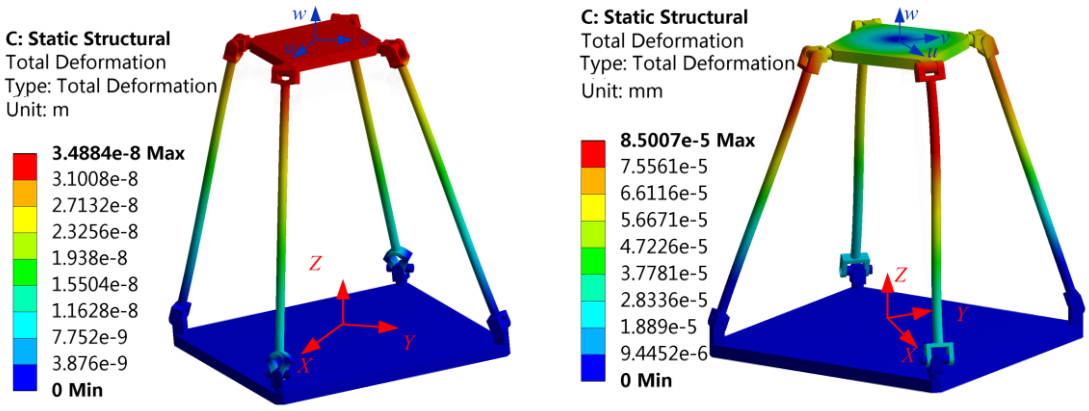

(c) Deformation along *Z*-axis under F=[0,0, 20N]^T (d) Deformation about *Z*-axis under M=[0,0, 20Nm]^T

Fig. 3. Deformation with force/moment imposed at the point *A*.

Based on the FEA analysis, the linear and angular stiffness can be numerically calculated by the ratio the fore or moment and the displacement or angle. Table II shows the comparison of the analytic model and the FEA model.

TABLE II: A COMPARISON WITH ANALYTIC METHOD AND FEA METHOD

Parameter	Analytic	FEA
k_x (N/um)	32.97	31.68
k_y (N/um)	32.97	30.89
k_z (N/um)	581.36	578.41
k_w x10^4 (Nm/rad)	8	7.86

It can be seen that the results from the analytic method match well with those evaluated by FEA method based on the hypotheses. Therefore, the established analytical model of the whole manipulator stiffness is effective and can be employed to evaluate the stiffness performance of the proposed manipulator.

For the purpose of analysis, a specified workspace is defined as $-40 \le \alpha \le 40$, $-40 \le \beta \le 40$, and z=853. Now the stiffness distributions of the PKM are illustrated in Fig.4.

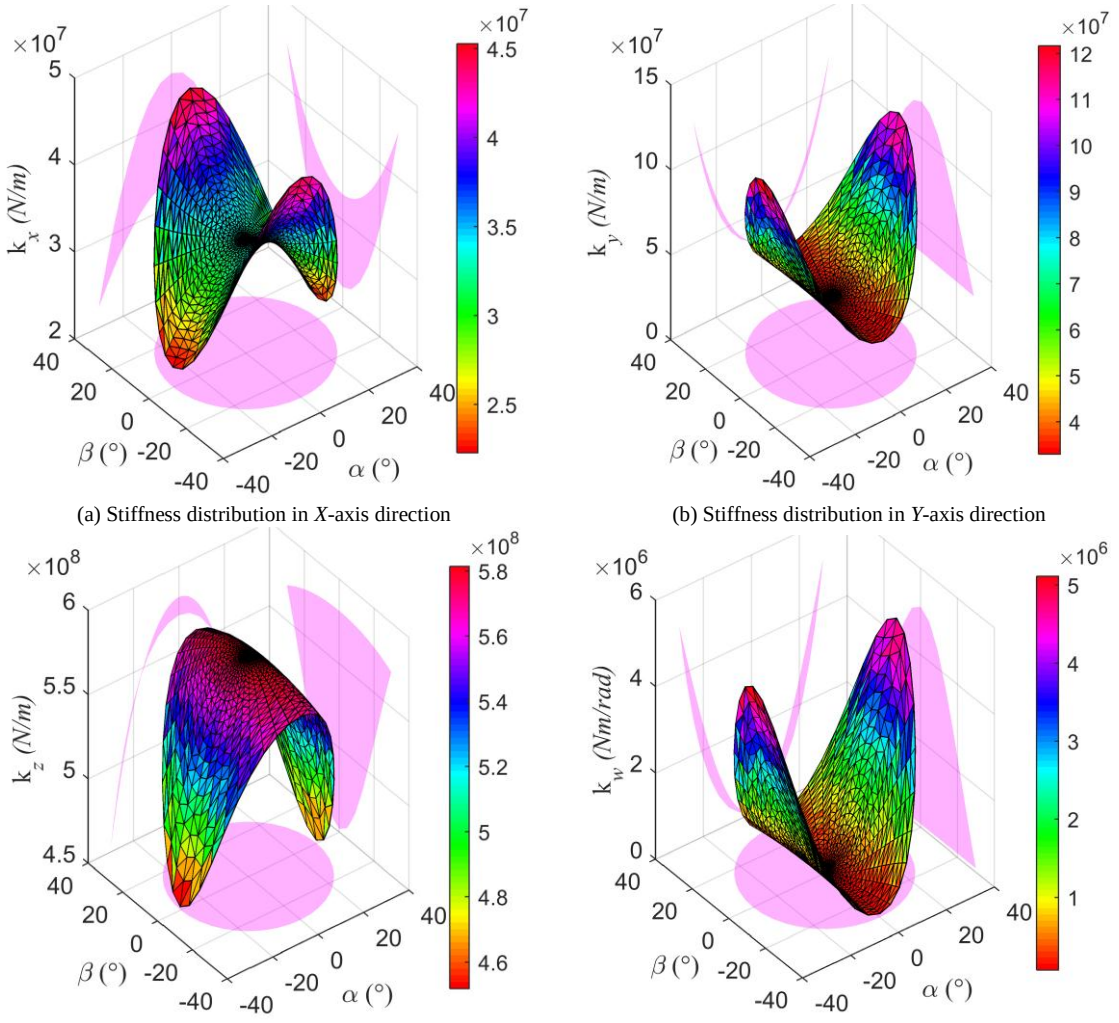

(a) Stiffness distribution in *X*-axis direction (b) Stiffness distribution in *Y*-axis direction

(c) Stiffness distribution in *Z*-axis direction (d) Stiffness distribution about *Z*-axis direction

Fig. 4. Stiffness distribution law in prescribed workspace.

As shown in Fig.4a-4d, the linear stiffness k_x and k_y are distributed axis-symmetrically in nature and the magnitude of k_x and k_y is very approximate, what's more, the linear stiffness in *z* direction is larger than that in *x* and *y*, which just satisfied the machining milling requirements for high position accuracy. Along with the varying of orientation parameters of the PKM, the tendency of variation on the linear stiffness in the workspace is decreased in Fig.4c. The variation of k_z is contrary to that of k_w.

B. Eigenscrew Decomposition of Stiffness Matrix

In the screw, the end deformation ΔX can be usually expressed in the axis coordinate system, while the wrench screw can be generally indicated in the ray coordinate system [23]-[25]. In order to ensure the consistency of the coordinate system, the twist screw and wrench screw are denoted in the same coordinate system, the axis coordinate system is converted to the ray coordinate system by employed the matrix, i.e. Δ, that is,

$$\Delta = \begin{bmatrix} \mathbf{0}_{3\times3} & \mathbf{I} \\ \mathbf{I} & \mathbf{0}_{3\times3} \end{bmatrix} \tag{28}$$

where $\mathbf{I}$ denotes an identity matrix, and the matrix Δ interchange the first and the last three elements.

Therefore, the decomposition of the stiffness matrix is converted into the decomposition of the matrix $\mathbf{K}\Delta$, that is,

$$\mathbf{K}\Delta e = \lambda e \tag{29}$$

where λ and e is the eigenvalues and the eigenvectors of the matrix $\mathbf{K}\Delta$ at a given position, respectively.

The eigenscrew decomposition of the stiffness matrix can be straightforward obtained as

$$\mathbf{K} = \sum_{m=1}^{6} k_m w_m w_m^{\mathrm{T}}, k_m = \frac{\lambda_m}{2h_m},$$
$$h_m = \frac{1}{2} w_m^{\mathrm{T}} \Delta w_m, w_m = \begin{bmatrix} n_m \\ \rho_m \times n_m + h_m n_m \end{bmatrix} \tag{30}$$

where k_m is the spring constant, e_m is the *m*-th eigenvector of the matrix $\mathbf{K}\Delta$, w_m is the unit screw of the eigenvector e_m, h_m expressed the pitch of vector w_m, n_m is the direction vector of the vector w_m, ρ_m is the position vector that w_m relative to the original coordinate system.

The eigenscrew decomposition is applied to the stiffness matrix K as described in Eq.(27). By sorting to solve the eigenscrew problem in Eq.(29), the six eigenstiffness λ_m, the six eigenscrew pitches h_m, and the six corresponding unit eigenscrew w_m can be derived in more detail in Eq.(31)

$$\begin{aligned} \lambda_m &= diag([-7.1231 \quad 7.1231 \quad -1.4493 \quad -1.3614 \quad 1.4493 \quad 1.3614]) \times 10^6 \\ h_m &= diag([-0.0135 \quad 0.0135 \quad -0.0431 \quad -0.0159 \quad 0.0431 \quad 0.0159]) \\ w_m &= \begin{bmatrix} -0.0780 & 0.0780 & 0.1239 & 0.5842 & 0.1239 & 0.5842 \\ 0.0096 & 0.0096 & 0.9828 & -0.0753 & -0.9828 & 0.0753 \\ 0.9969 & -0.9969 & 0.1371 & 0.8081 & 0.1371 & 0.8081 \\ 0.0090 & 0.0090 & -0.8158 & 0.0379 & 0.8158 & -0.0379 \\ -0.0644 & 0.0644 & 0.0590 & 0.4852 & 0.0590 & 0.4852 \\ -0.0122 & -0.0122 & -0.003 & -0.0019 & 0.003 & 0.0019 \end{bmatrix} \end{aligned} \tag{31}$$

The interpretation of stiffness matrix K based on eigenscrew decomposition is elaborated in Table III, which indicates that stiffness matrix K can be interpreted by a body suspended by six-dimensional screw springs with directions along the eigenscrew of the stiffness matrix K as shown in Fig. 5. p_m denotes the pitch of helical joint used in the screw spring.

TABLE III: THE EQUIVALENT SCREW SPRING

Springs	$k_m / \times 10^8$	n_m	ρ_m	$p_m \ (-2\pi h_m)$
1	2.6401	[-0.0780, 0.0096, 0.9969]$^{\mathrm{T}}$	[0.0640, 0.0080, 0.0049]$^{\mathrm{T}}$	0.0848
2	2.6401	[0.0780, 0.0096, -0.9969]$^{\mathrm{T}}$	[0.0640, -0.0080, 0.0049]$^{\mathrm{T}}$	-0.0848
3	0.1679	[0.1239, 0.9828, 0.1371]$^{\mathrm{T}}$	[-0.0084, -0.1118, 0.8091]$^{\mathrm{T}}$	0.2711
4	0.4286	[0.5842, -0.0753, 0.8081]$^{\mathrm{T}}$	[-0.3920, 0.0318, 0.2863]$^{\mathrm{T}}$	0.0988
5	0.1679	[0.1239, -0.9828, 0.1371]$^{\mathrm{T}}$	[-0.0084, 0.1118, 0.8091]$^{\mathrm{T}}$	-0.2711
6	0.4286	[0.5842, 0.0753, 0.8081]$^{\mathrm{T}}$	[-0.3920, -0.0318, 0.2863]$^{\mathrm{T}}$	-0.0988

From the Table III and Fig. 5, we can see that the eigenscrew decomposition of the stiffness matrix can be deduced into six simple screw springs superimposition, and dived into three groups of springs. Each group has two springs at one common point with the same spring stiffness, and the pitch is opposite. Since the parallel manipulator own two different chains, the manipulator doesn't exhibit one certain symmetry, and the distribution of the springs is not regular.

C. The Maximum and Minimum Eigenvalue of Stiffness Matrix

In order to evaluate the stiffness value of some positions in prescribed workspace, the maximum and minimum eigenvalues of the stiffness matrix $\mathbf{K}$ are usually employed as the evaluation indices of parallel kinematic machine.

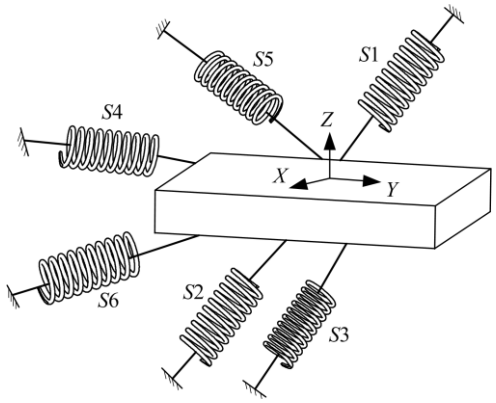

Fig. 5. The physical interpretation of the stiffness of the PKM.

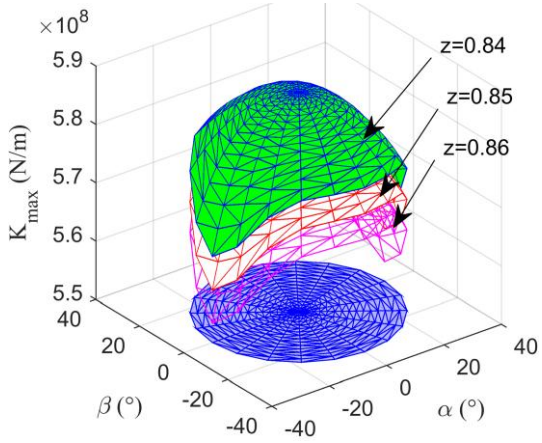

Fig. 6. The maximum eigenvalue of the stiffness matrix.

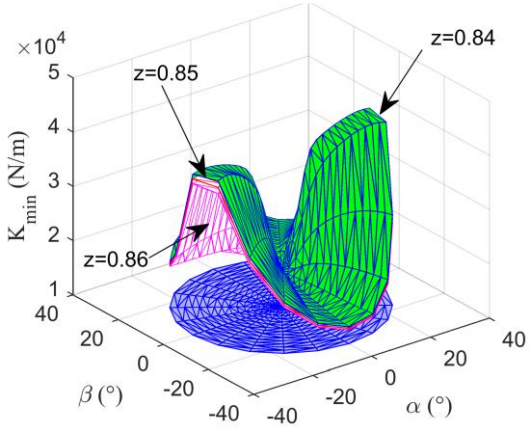

Fig.7. The minimum eigenvalue of the stiffness matrix.

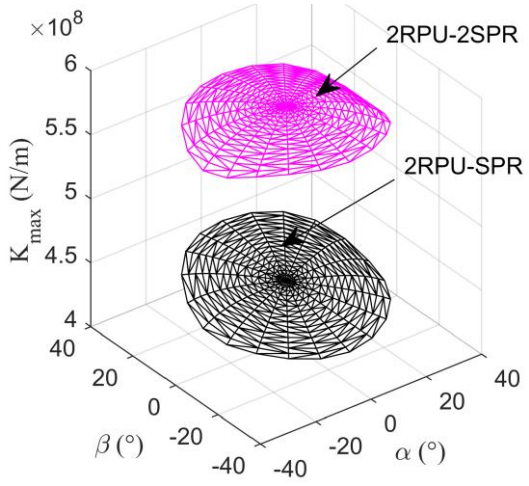

Fig. 8. The maximum eigenvalue of the stiffness matrix.

Fig. 6 and Fig. 7 illustrated the atlas of the maximum value and the minimum value of the 2RPU-2SPR parallel manipulator with different height in prescribed workspace, from the figures, the maximum and minimum eigenvalues of the stiffness matrix decreased with the increment of z. The lowest highest value of maximum stiffness occurs around the boundary of the workspace, so does the highest value of the minimum stiffness, since the manipulator approaches singular when it comes near the workspace boundary.

The preliminary comparison between the redundantly actuated and overconstrained 2RPU-2SPR parallel manipulator and the 2RPU-SPR parallel manipulator without actuation redundancy illustrates that the former own higher stiffness than that of the latter in a same positions as shown in Fig.8. In terms of the engineering application of machining milling, the proposed manipulator has better stiffness values and exhibits desirable stiffness characteristics to satisfy the requirements for high position accuracy

VI. Conclusion

In order to accomplish the high-speed machining of aerospace structural components with large dimension and with complex freedom surface, this paper proposed a novel 1T2R redundantly actuated and overconstrained parallel kinematic machine tool, which can integrate two X-Y tracks to construct a five axis hybrid machine tool. From the investigation, the following conclusions can be drawn:

(1) The actuation force and constraint force/moment of the proposed manipulator are analyzed in detail by sorting to the screw theory, and the freedom of the parallel manipulator is further determined.

(2) The stiffness model of the redundantly actuated and over-constrained parallel manipulator was formulated under the hypothesis that the main deformation sources are concentrated on the links by simultaneously considering the actuation and constraints force, and this theoretical model is verified by the FEA simulation method.

(3) The stiffness distributions of the proposed manipulator are illustrated. The algebraic characteristics such as the linear stiffness, angular stiffness, eigenvalue and eigenscrew of the stiffness matrix are usually employed as the performance index to evaluate the stiffness of the parallel manipulator. The results indicate the proposed manipulator has much higher stiffness than the 2RPU-SPR parallel manipulator without actuation redundancy, which is a great merit and has wide engineering applications in the fields of industrial robot and parallel kinematics machine tools. For the further work, more performance induces such as dexterity, motion-force transmission, kinematic accuracy and reliability will be considered to enhance the ability of the proposed parallel kinematic machine, and then a real-prototype will be fabricated.

Acknowledgment

This research is sponsored by the Fundamental Research Funds for the Central Universities under Grant No.2017YJS158.

REFERENCES

[1] N. Hennes and D. Staimer, "Application of PKM in aerospace manufacturing-high performance machining centers ECOSPEED, ECOSPEED-F and ECOLINER," in *Proc. 4th Chemnitz Parallel Kinematics Seminar*, Chemnitz, Germany, 2004, pp. 557–77.

[2] B. Siciliano, "The Tricept robot: Inverse kinematics, manipulability analysis and closed-loop direct kinematics algorithm," Cambridge University Press, vol.197, no. 4, pp. 437-445, 1999.

[3] Z. M. Bi and Y. Jin, "Kinematic modeling of Exechon parallel kinematic machine," *Robotics and Computer Integrated Manufacturing*, vol. 27, no. 1, pp. 186-193,2011.

[4] H. T. Liu, T. Huang, and A. Kecskeméthy, "Force/motion transmissibility analyses of redundantly actuated and overconstrained parallel manipulators," *Mechanism and Machine Theory*, vol. 109, pp.126-138, 2017.

[5] B. Hu and Z. Huang, "Kinetostatic model of overconstrained lower mobility parallel manipulators," *Nonlinear Dynamics*, vol. 86, no. 1, pp. 309-322, 2016.

[6] X. Liu, Y. Xu, and J. Yao, "Control-faced dynamics with deformation compatibility for a 5-DOF active over-constrained spatial parallel manipulator 6PUS–UPU," *Mechatronics*, vol. 30, pp. 107-115, 2015.

[7] C. M. Gosselin, "Stiffness mapping for parallel manipulators," *IEEE Transactions on Robotics and Automation*, vol. 6, no. 3, pp. 377-382, 1990.

[8] C. M. Clinton, G. M. Zhang, and A. J. Wavering, "Stiffness modeling of a stewart-platform-based milling machine," *Transaction of NAMRI/SME*, vol.115, pp. 335-340, 1997.

[9] R. G. Robert, "Minimal realization of an arbitrary spatial stiffness matrix with a parallel connection of simple and complex springs," *IEEE Transactions on Robotics and Automation*, vol. 16, no. 5, pp. 603-608,2000.

[10] Y. Zhao, Y. Jin, and J. Zhang, "Kinetostatic modeling and analysis of an exechon parallel kinematic machine (PKM) module," *Chinese Journal of Mechanical Engineering*, vol. 29, no. 1, pp. 33-44, 2016.

[11] D. Zhang, C. M. Gosselin, "Kinetostatic modeling of n-dof parallel mechanisms with a passive constraining leg and prismatic actuators," *ASME Journal of Mechanical Design*, vol.123, no. 3, pp. 375-384, 2001.

[12] E. Khasawneh and P. M. Ferreira, "Computation of stiffness and stiffness bounds for parallel link manipulators," *International Journal of Machine Tools and Manufacture*, vol. 39, no. 2, pp. 321-342,1999.

[13] Y. Wang, H. Liu, and T. Huang, "Stiffness modeling of the Tricept robot using the overall Jacobian matrix," *ASME Journal of Mechanisms and Robotics*, vol. 1, no.2, pp. 021002.1-021002.8,2009.

[14] Q. Yan, B. Li, and Y. Li, "Kinematics comparative study of two overconstrained parallel manipulators," *Mathematical Problems in Engineering*, vol. 6, pp. 1-12, 2016.

[15] J. Zhang, Y. Zhao, and Y. Jin, "Elastodynamic modeling and analysis for an exechon parallel kinematic machine," *Journal of Manufacturing Science and Engineering*, vol. 138, no. 3, pp. 1-14, 2016.

[16] X. L. Cui, W. Y. Chen, and X. G. Han, "Stiffness improvement of 3RPS PKM by Redundant actuating leg," *Chinese Journal of Mechanical Engineering*, vol.26, no.23,pp.3162-3167,2015.

[17] Y. S. Zhao, Y. D. Xu, and J. T. Yao, "A force analysis method for overconstrained parallel mechanisms," *Chinese Journal of Mechanical Engineering*, vol. 25, no.6, pp.711-717, 2014.

[18] Z. Huang, J. F. Liu, and D. X. Zeng, "A general methodology for mobility analysis of mechanisms based on constraint screw theory," *Science in China Series E: Technological Sciences*, vol. 52, no. 5, pp.1337-1347, 2009.

[19] Y. Lu, X. Zhang, and C. Sui, "Kinematics/statics and workspace analysis of a 3-leg 5-DoF parallel manipulator with a UPU-type composite active constrained leg," *Robotica*, vol. 31, no. 2, pp.183-191, 2013.

[20] H. Nigatu and M. Gurala, "Dynamic and stiffness modeling of new 3DOF PKM for high speed machining application," *International Journal of Engineering and Technology Sciences*, vol.3, pp.2308-2315, 2014.

[21] Y. G. Li, H. T. Liu, and X. M. Zhao, "Design of a 3-DOF PKM module for large structural component machining," *Mechanism and Machine Theory*, vol. 45, no. 6, pp. 941-954, 2010.

[22] K. K. Kumar, A. Srinath, and B. Siddhartha, "Simulation and analysis of parallel manipulator for manoeuvring laparoscopic camera-CAD based approach," *International Journal of Engineering and Technology*, vol. 7, no. 1, pp. 294-302, 2015

[23] Y. Li and Q. Xu, "Stiffness analysis for a 3-PUU parallel kinematic machine," *Mechanism and Machine Theory*, vol.43, no.2, pp.186-200, 2008.

[24] S. Huang and J. M. Schimmels, "The eigenscrew decomposition of spatial stiffness matrices," *IEEE Transactions on Robotics and Automation*, vol.16, no. 2, pp. 146-156, 2000.

[25] G. Chen, H. Wang, and Z. Lin, "The principal axes decomposition of spatial stiffness matrices," *IEEE Transactions on Robotics*, vol. 31, no.1, pp. 191-207, 2015

Haiqiang Zhang is a PhD student in the school of Beijing Jiaotong University, Beijing, China from 2015. He was born in 1986. He received the master degree in mechanical engineering from Hebei University of Engineering in 2015 and the bachelor degree in mechanical design and theories from Yantai University in 2012. His primary research interest is focus on robotics in computer integrated manufacturing, parallel kinematics machine tool, redundant actuation robots, overconstrained parallel manipulators, and multi-objective optimization design, etc.

Hairong Fang received the bachelor degree in mechanical engineering from Nanjing University of Science and Technology in 1990, master degree in mechanical engineering from Sichuan University in 1996, and PhD degree in mechanical engineering from Beijing Jiaotong University in 2005, respectively. She worked as an assistant professor in the Department of Engineering Mechanics at Beijing Jiaotong University, Beijing, China, from 2010 to now. Currently, she is a full professor in the School of Mechanical Engineering and Director of Robotics Research Center. Her primary research interests in parallel mechanisms, digital control, robotics and automation, machine tool equipment, and green manufacturing.